Modular matrices from universal wave-function overlaps in Gutzwiller-projected parton wave functions

Jia-Wei Mei[1] and Xiao-Gang Wen[1,2]

[1]*Perimeter Institute for Theoretical Physics, Waterloo, Ontario, Canada N2L 2Y5*

[2]*Department of Physics, Massachusetts Institute of Technology, Cambridge, Massachusetts 02139, USA*

(Received 6 October 2014; revised manuscript received 22 February 2015; published 12 March 2015)

We implement the universal wave-function overlap (UWFO) method to extract modular S and T matrices for topological orders in Gutzwiller-projected parton wave functions (GPWFs). The modular S and T matrices generate a projective representation of $SL(2,\mathbb{Z})$ on the degenerate-ground-state Hilbert space on a torus and may fully characterize the 2+1D topological orders, i.e., the quasiparticle statistics and chiral central charge (up to E_8 bosonic quantum Hall states). We use the variational Monte Carlo method to computed the S and T matrices of the chiral spin liquid (CSL) constructed by the GPWF on the square lattice, and we confirm that the CSL carries the same topological order as the $\nu = \frac{1}{2}$ bosonic Laughlin state. We find that the nonuniversal exponents in the UWFO can be small, and direct numerical computation can be applied on relatively large systems. The UWFO may be a powerful method to calculate the topological order in GPWFs.

DOI: 10.1103/PhysRevB.91.125123 PACS number(s): 75.10.Kt, 05.30.Pr, 73.43.−f

Topological order [1–3] connotes the pattern of long-range entanglement in gapped many-body wave functions [4–6]. It describes gapped quantum phases of matter that lie beyond the Landau symmetry breaking paradigm [7]. Local unitary transformations on many-body wave functions can remove local entanglement, however they preserve long-range topological entanglement. Therefore, a topological ordered state is not smoothly connected to a trivial (direct product) state by local unitary transformations [6]. Physically, topological order is described through topological quantum numbers, such as nontrivial ground-state structures and fractional excitations [1–3,8–10]. These topological properties are fully characterized by the quasiparticle (anyon in the bulk) statistics [8–10] and the chiral central charge, which encodes information about chiral gapless edge states [11,12].

Both the fusion rule and the topological spin of quasiparticles as well as the chiral central charge are characterized in the non-Abelian geometric phases encoded in the degenerate ground states [1–3,13–17], and vice versa. The non-Abelian geometric phases form a representation of $SL(2,\mathbb{Z})$ that is generated by 90° rotation and Dehn twist on a torus; they are called modular S and T matrices, respectively [13,14]. The element of the modular S matrix determines the mutual statistics of quasiparticles, while the element of the T matrix determines the topological spin $\theta_a \in U(1)$ and the chiral central charge [1,13,14].

Given the fusion coefficients N_c^{ab} and the topological spin θ_a, we can write down the modular S and T matrices as the following expressions: $S_{ab} = \frac{1}{\mathcal{D}} \sum_c N_c^{a\bar{b}} \frac{\theta_c}{\theta_a \theta_b} d_c$ and $T_{ab} = e^{-i\frac{2\pi c}{24}} \theta_a \delta_{a,b}$ [18]. Here d_a (called the quantum dimension of quasiparticle a) is the largest eigenvalue of matrix N_a, which is defined as $(N_a)_{bc} = N_c^{ab}$, and $\mathcal{D}$ is the total quantum dimension, $\mathcal{D}^2 = \sum_a d_a^2$. We see that $S_{a1} = \frac{d_a}{\mathcal{D}}$.

From the Verlinde formula [19], we can reconstruct the fusion coefficients, $N_{ab}^c = \sum_x \frac{S_{ax} S_{bx} S_{cx}^*}{S_{1x}}$. Therefore, S and T provide a complete description and can be taken as the order parameter of topological orders [14–17]. The modular S and T matrices satisfy the relations $(ST)^3 = C$ and $S^2 = C$, where C is a so-called charge conjugation matrix that satisfies $C^2 = 1$. The central charge c determines the thermal current of the edge state, $I_E = \frac{c}{6} T^2$, at temperature T [20] and is fixed up to E_8 bosonic quantum Hall states.

To fully characterize topological order, various numerical methods are proposed to access the modular S and T matrices from ground-state wave functions [21–26]. By braiding quasiholes, the modular S and T can be extracted from the Berry matrices [27–29]. Recently, one of us proposed the universal wave-function overlap (UWFO) method to calculate modular matrices [16,30]. For a given set $\{|\psi_a\rangle\}_{a=1}^N$ of degenerate ground-state wave functions, it provides us with a practical method to extract the modular S and T matrices,

$$\begin{aligned} \tilde{S}_{ab} &= \langle \psi_a | \hat{S} | \psi_b \rangle = e^{-\alpha_S L^2 + o(1/L^2)} S_{ab}, \\ \tilde{T}_{ab} &= \langle \psi_a | \hat{T} | \psi_b \rangle = e^{-\alpha_T L^2 + o(1/L^2)} T_{ab}, \end{aligned} \tag{1}$$

where $\hat{S}$ and $\hat{T}$ are the operators that generate the 90° rotation and Dehn twist, respectively, on a torus with the L^2 lattice size. The exponentially small prefactor makes it difficult to numerically calculate the UWFO in (1). To avoid the exponential smallness, a gauge-symmetry preserved tensor renormalization method has been developed for the tensor-network wave functions [16,17], where the system size is effectively reduced as zero after the tensor renormalization.

Actually, in this paper, we will show that the nonuniversal exponent $\alpha_{T,S}$ can be small such that the UWFO can be directly numerically calculated on relatively large systems. We will take a chiral spin liquid (CSL) wave function on the square lattice [31] as an explicit example to extract the modular S and T matrices from the UWFO. We construct the set of ground states for a CSL by using Gutzwiller-projected parton wave functions (GPWF) [21,31–34]. We use the variational Monte Carlo method to calculate the UWFO for the CSL wave functions. The hopping parameters are set as $|t_1/t_0| = 0.5$ for the CSL on the π-flux square lattice, where t_0 and t_1 for nearest-neighbor and next-nearest-neighbor links, respectively. Due to C_4 symmetry, the overlap $\tilde{S}$ in Eq. (1) has a vanishing exponent $\alpha_S = 0$. $\tilde{T}$ in Eq. (1) has the relatively small nonuniversal complex exponent $\alpha_T = 0.042\,08 + 0.4809i$, and the direct

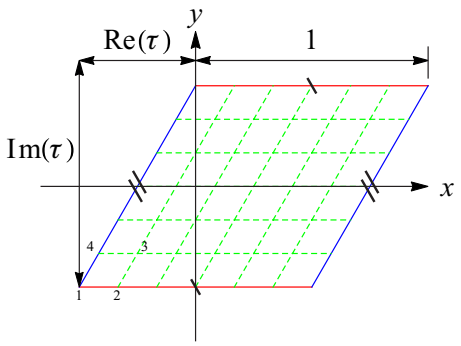

FIG. 1. (Color online) The lattice system can be put on a torus by imposing the equivalence conditions $z \sim z+1$ and $z \sim z+\tau$, where $\tau = \tau_x + i\tau_y$ is a complex number. The principal region of a torus is bounded by the four points $z = \frac{1}{2}(\pm 1 \pm \tau)$. Here the top and bottom and left and right sides are identified, respectively.

numeric computation is carried out on relatively large systems up to a 12×12 lattice size in this paper. The CSL is the lattice analogy of the $\nu = \frac{1}{2}$ bosonic Laughlin state [31,32]. The parent Hamiltonians for CSL are also proposed in Refs. [35,36]. Our numerical results confirm the analogy by directly extracting the modular S and T matrices from the UWFO.

In the parton construction, the $S = \frac{1}{2}$ spin operator is written in terms of fermionic parton operators, $S^a(z_i) = \frac{1}{2} f^\dagger_\sigma(z_i)\sigma^a_{\sigma\sigma'} f_{\sigma'}(z_i)$. Here σ^a $(a = x,y,z)$ is the Pauli matrices and $f_{i\sigma}$ $(\sigma = \uparrow/\downarrow)$ is the fermionic parton operator. We take the complex variables for the i-site coordinate, $z_i = x_i + iy_i$, on a lattice. We have to impose the one-particle-per-site constraint for the partons, $f^\dagger_\uparrow(z_i)f_\uparrow(z_i) + f^\dagger_\downarrow(z_i)f_\downarrow(z_i) = 1$, such that the fermionic partons have the same Hilbert space on the i-site as the spin operators $S^a(z_i)$. The GPWF for the spin system can be read as

$$|\Psi\rangle = \sum_{\{z_i\}} \mathcal{P}_G \Psi(\{z_i^\uparrow, z_k^\downarrow\})|\{z_i\}\rangle, \tag{2}$$

where $|\{z_i\}\rangle$ is the spin configuration and $\mathcal{P}_G$ is the Gutzwiller projection operator to impose the one-particle-per-site constraint for the fermionic partons.

The GPWF can be put on a torus by implying the equivalence conditions $z \sim z+1$ and $z \sim z+\tau$, as shown in Fig. 1. The principal region of a torus is bounded by the four points $z = \frac{1}{2}(\pm 1 \pm \tau)$. The torus is defined by two primitive vectors $\vec{\omega}_1 = 1$ and $\vec{\omega}_2 = \tau_x + i\tau_y$. The shape of the torus is invariant under the $SL(2,\mathbb{Z})$ transformations $\begin{pmatrix}\vec{\omega}'_1\\ \vec{\omega}'_2\end{pmatrix} = M\begin{pmatrix}\vec{\omega}_1\\ \vec{\omega}_2\end{pmatrix}$ with $M \in SL(2,\mathbb{Z})$, and the generators ($\hat{S}$ and $\hat{T}$) have the expressions

$$\hat{S} = \begin{pmatrix}0 & -1\\ 1 & 0\end{pmatrix}, \quad \hat{T} = \begin{pmatrix}1 & 1\\ 0 & 1\end{pmatrix}. \tag{3}$$

Two different constructions of GPWF for a CSL in the lattice analogy of the $\nu = \frac{1}{2}$ bosonic Laughlin state can be found in Refs. [31,32]. In Ref. [32], the parton wave functions are discretized integer quantum Hall states and we call it the *ideal* GPWF for a CSL. On a torus, we can explicitly write down the ideal GPWF in terms the Laughlin-Jastrow wave functions [37],

$$\begin{aligned}\mathcal{P}_G\Psi(\{z_i^\uparrow, z_k^\downarrow\}) &= e^{i\frac{K^\uparrow - K^\downarrow}{2}(Z^\uparrow - Z^\downarrow)}\vartheta_{\frac{1}{2},\frac{1}{2}}(Z^\uparrow - Z_0^\uparrow|\tau)\vartheta_{\frac{1}{2},\frac{1}{2}}(Z^\downarrow - Z_0^\downarrow|\tau)\\ &\times \mathcal{P}_G \prod_{i<j}^{N^\uparrow}\vartheta_{\frac{1}{2},\frac{1}{2}}(z_i^\uparrow - z_j^\uparrow|\tau)\prod_{k<l}^{N^\downarrow}\vartheta_{\frac{1}{2},\frac{1}{2}}(z_k^\downarrow - z_l^\downarrow|\tau),\end{aligned} \tag{4}$$

where $\theta_{a,b}(z|\tau)$ is the theta function and $Z^\sigma = \sum_i z_i^\sigma$ is the center-of-mass coordinate. Different ground states are specified by the different zeros, Z_0^σ, in the center-of-mass wave functions. The zeros are determined by the general boundary conditions [37,38]. The modular S and T matrices for the ideal GPWF in Eq. (4) can be analytically calculated by deformation of the mass matrix [14],

$$S = \frac{1}{\sqrt{2}}\begin{pmatrix}1 & 1\\ 1 & -1\end{pmatrix}, \quad T = e^{-i\frac{2\pi c}{24}}\begin{pmatrix}1 & 0\\ 0 & e^{i\frac{\pi}{2}}\end{pmatrix} \tag{5}$$

with the central charge $c = 1$, the same as those for the $\nu = \frac{1}{2}$ bosonic Laughlin state.

In Ref. [31], the *generic* GPWF for a CSL is written as

$$\mathcal{P}_G\Psi(\{z_i^\uparrow, z_i^\downarrow\}) = \mathcal{P}_G \det\varphi_i(z_j^\uparrow)\det\varphi_k(z_l^\downarrow), \tag{6}$$

where $\det\varphi_i(z_j^{\uparrow/\downarrow})$ is the determinate wave function for the fermionic partons filling the valence bands of the tight-binding model,

$$H_{\mathrm{MF}} = -\sum_{ij,\sigma} t(z_i,z_j) f^\dagger_\sigma(z_i) f_\sigma(z_j) + \mathrm{H.c.}, \tag{7}$$

on the π-flux square lattice with both nearest-neighbor and next-nearest-neighbor hopping amplitude [31]. There are $\frac{\pi}{2}$ fluxes in every triangle in the plaquette, e.g., $\triangle_{123}$ in $\square_{1234}$ in Fig. 1, $\Phi(\triangle_{123}) = \arg(t_{z_1z_2}t_{z_2z_3}t_{z_3z_1}) = \frac{\pi}{2}$. Different ground-state wave functions can be obtained by different general boundary conditions. For the spin operator, the boundary condition is

$$S^+(z_i+1) = e^{i\Phi^s_1}S^+(z_i), \quad S^+(z_i+\tau) = e^{i\Phi^s_2}S^+(z_i).$$

Due to fractionalization in the GPWF [39,40], the parton has the boundary condition

$$f^\dagger_\sigma(z_i+1) = e^{i\frac{\sigma}{2}\Phi^s_1}f^\dagger_\sigma(z_i), \quad f^\dagger_\sigma(z_i+\tau) = e^{i\frac{\sigma}{2}\Phi^s_2}f^\dagger_\sigma(z_i),$$

with $\sigma = \pm 1$ for $f^\dagger_{\uparrow/\downarrow}$. When we increase $\Phi^s_{1,2}$ from 0 to 2π, the spin operators are invariant, however the parton wave functions do not go back to themselves and lead to another ground state for the GPWF. Therefore, we have different ground states for a CSL labeled by the spin fluxes in the holes of a torus $|\Phi^s_1, \Phi^s_2\rangle$,

$$\{|\Psi_a\rangle\} = \{|0,0\rangle, |0,2\pi\rangle, |2\pi,0\rangle, |2\pi,2\pi\rangle\}, \tag{8}$$

with $a = 1,2,3,4$. Actually only two of them are linearly independent.

For the generic GPWF in Eq. (6), we use the UWFO in Eq. (1) to exact the modular matrices S and T. To carry out the UWFO, we need calculate the following overlaps:

$$P_{ab} = \langle\Psi_a|\Psi_b\rangle, \quad \tilde{S}_{ab} = \langle\Psi_a|\Psi^S_b\rangle, \quad \tilde{T}_{ab} = \langle\Psi_a|\Psi^T_b\rangle, \tag{9}$$

where $|\Psi_a\rangle$ is the state in Eq. (8) and $|\Psi^S_b\rangle = \hat{S}|\Psi_b\rangle$, $|\Psi^T_b\rangle = \hat{T}|\Psi_b\rangle$, where $\hat{S}$ and $\hat{T}$ are the 90° rotation and Dehn twist

transformations in Eq. (3) on a torus. The P matrix has rank 2 with the numerical tolerance less than 10^{-3} implying twofold ground-state degeneracy.

Given GPWFs, we implement the "sign trick" [41] to calculate the overlap,

$$\langle\Psi_a|\Psi_b\rangle = \sum_{\{z_i\}} \psi_a^*(\{z_i\})\psi_b(\{z_i\}) \equiv \langle\Psi_a|\Psi_b\rangle_{\rm amp}\langle\Psi_a|\Psi_b\rangle_{\rm sgn}, \quad (10)$$

where $\psi_a(\{z_i\})$ is the amplitude wave function of the spin configuration $\{z_i\}$ in $|\Psi_a\rangle$, and the sign term

$$\langle\Psi_a|\Psi_b\rangle_{\rm sgn} = \sum_{\{z_i\}} \rho_{ab} \frac{\psi_a^*(\{z_i\})\psi_b(\{z_i\}}{|\psi_a(\{z_i\})\psi_b(\{z_i\})|} \quad (11)$$

is calculated using the Monte Carlo method according to the weight $\rho_{ab} = |\psi_a(\{z_i\})\psi_b(\{z_i\})|$. The amplitude term is the normalization factor for weight ρ_{ab},

$$\langle\Psi_a|\Psi_b\rangle_{\rm amp} = \sum_{\{z_i\}} |\psi_a(\{z_i\})\psi_b(\{z_i\})|. \quad (12)$$

Actually, we are only interested in the ratios of amplitudes. For example, for the P matrix in Eq. (9), we evaluate the matrix-element amplitude ratios

$$\frac{\langle\Psi_a|\Psi_b\rangle_{\rm amp}}{\langle\Psi_1|\Psi_1\rangle_{\rm amp}} = \frac{\sum_{\{z_i\}} \rho_{ab;11}\sqrt{|\frac{\psi_a(\{z_i\})\psi_b(\{z_i\})}{\psi_1(\{z_i\})\psi_1(\{z_i\})}|}}{\sum_{\{z_i\}} \rho_{ab;11}\sqrt{|\frac{\psi_1(\{z_i\})\psi_1(\{z_i\})}{\psi_a(\{z_i\})\psi_b(\{z_i\})}|}} \quad (13)$$

according to the Monte Carlo sampling weight $\rho_{ab;11} = \sqrt{|\psi_a(\{z_i\})\psi_b(\{z_i\})\psi_1(\{z_i\})\psi_1(\{z_i\})|}$.

We set the mean-field hopping parameters as $t_1/t_0 = 0.5$, where t_0 and t_1 are for nearest-neighbor and next-nearest-neighbor links, respectively. The overlap calculations are carried out on the systems with $L \times L$ lattice sizes, $L = 6,8,10,12$. From the overlaps in Eq. (9), we follow the steps below to extract the modular S and T matrices. We first diagonalize the P matrix,

$$P = U^\dagger P_\Lambda U, \quad U = (u_1,u_2,u_3,u_4). \quad (14)$$

Only two eigenvectors (e.g., u_3 and u_4) have nonzero eigenvalues around 2. These two states (u_3 and u_4) are the linearly independent ground sates. In terms of the normalized $\tilde{U} = (u_3,u_4)$, the overlaps for $\tilde{S}$ and $\tilde{T}$ in Eq. (9) turn out to be 2×2 square matrices,

$$S^1_{2\times2} = \tilde{U}^\dagger \tilde{S}_{4\times4}\tilde{U}, \quad T^1_{2\times2} = \tilde{U}^\dagger \tilde{T}_{4\times4}\tilde{U}. \quad (15)$$

Generally, T^1 is not diagonal since u_3 and u_4 are not the minimum entangled states or eigenstates of the Wilson loop operators [21]. We then diagonalize T_1 to obtain the minimum entangled states v_1 and v_2,

$$T^1 = V^\dagger T' V, \quad S^1 = V^\dagger S' V, \quad V = (v_1,v_2), \quad (16)$$

where T' is diagonal and the phases of V are fixed according to the conditions $S'_{12} = S'_{21}$ and $S'_{1i} > 0$.

Since the CSL wave function has 90° rotation symmetry, the exponent in S' in Eq. (16) vanishes, $\alpha_S = 0$, which is confirmed in the numerical calculations. The UWFO of the T matrix has a complex exponent α_T in the prefactor. The real part of the exponent $\mathrm{Re}(\alpha_T)$ is easily obtained from the amplitude of the

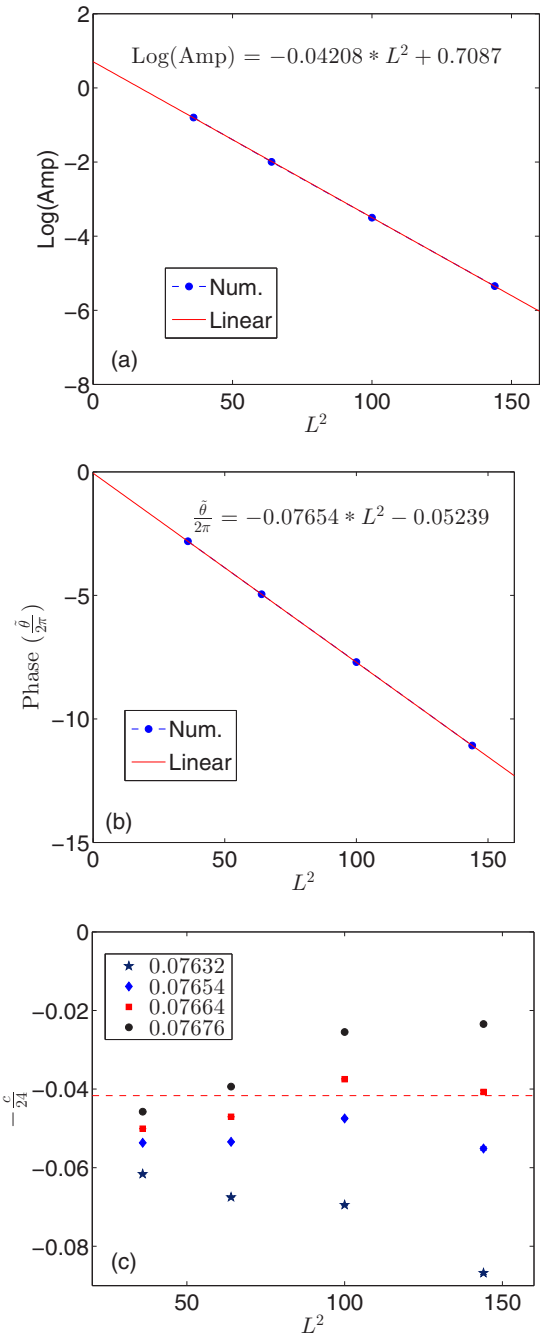

FIG. 2. (Color online) L^2-dependent of amplitude and phase of T' in Eq. (16) are shown in (a) and (b), respectively. Here $\mathrm{Log(Amp)} \equiv \log(|T'_{11}|)$ and $\frac{\tilde{\theta}}{2\pi} \equiv \frac{\arg T'_{11}}{2\pi} + k$ with $k = 3,5,8,11$ for $L = 6,8,10,12$. In (c), we plot $-\frac{c}{24} = \frac{\arg(T'_{11})}{2\pi} + \frac{\mathrm{Im}(\alpha_T)}{2\pi}L^2 \mod 1$ with different $\frac{\mathrm{Im}(\alpha_T)}{2\pi} = 0.07632,0.07654,0.07664,0.07676$. The red dashed line is for $c = 1$. In (c), the numerical error bars are included and smaller than the symbols' sizes.

T' in Eq. (16) by fitting $\log(\mathrm{amp}) \equiv \log(|T'_{11}|)$ with respect to L^2, $\mathrm{Re}(\alpha_T) = 0.042\,08$, as shown in Fig. 2(a). The phase $\tilde{\theta}$ is defined up to 2π, $\frac{\tilde{\theta}}{2\pi} \equiv \frac{\arg(T'_{11})}{2\pi} + k = -\frac{\mathrm{Im}(\alpha_T)}{2\pi}L^2 - \frac{c}{24}$ with $k \in \mathbb{Z}$. For $L = 6,8,10,12$, the corresponding integers are $k = 3,5,8,11$. From the fitting in Fig. 2(b), we obtain $\mathrm{Im}(\alpha_T) = 0.4809$. The central charge is sensitive to the exact value of

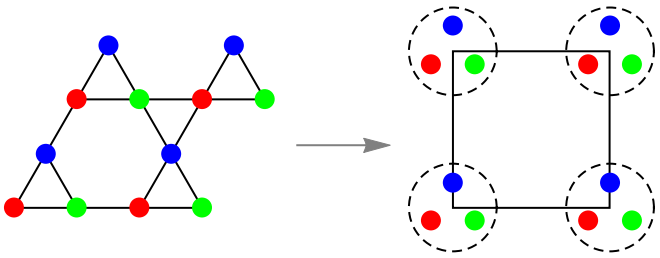

FIG. 3. (Color online) The kagome lattice is mapped onto a square lattice with three orbitals per site.

$\mathrm{Im}(\alpha_T)$ as shown in Fig. 2(c). The final result for the modular S and T matrices is

$$S = \begin{pmatrix} 0.714 & 0.707 \\ 0.707 & -0.698 \end{pmatrix}, \quad T = e^{-i\frac{2\pi c}{24}} \begin{pmatrix} 1 & 0 \\ 0 & e^{i0.501\pi} \end{pmatrix}, \quad (17)$$

with the central charge $c \simeq 1.25 \pm 0.5$, very close to the exact result for the ideal GPWF in Eq. (5).

Above we apply the UWFO method on the square lattice. For a general Bravais lattice, we can first map it onto an equivalent square lattice. We take the kagome lattice as an example. We map the unit cell of the kagome lattice onto the one with square unit cell. Different sites within the unit cell are mapped onto different orbitals on the square lattice, as shown in Fig. 3. Then we can make the modular transformations $\hat{S}$ and $\hat{T}$ on the square lattice torus. For systems without 90° rotation symmetry, the exponents $\alpha_{S,T}$ in Eq. (1) are both finite. On the square lattice, we can also use the Kadanoff block renormalization procedure to reduce the system size $L^2 \to \tilde{L}^2$. Then the exponents in the prefactors of the UWFO can be significantly reduced. Many local unitary transformations on the lattice can potentially reduce the exponents in the UWFO. If different ground-state sectors have the same topological spins, we can follow Ref. [15] to identify the minimum entangled states to diagonalize the modular T matrix. The UWFO method is easily generalized to the 3+1D topological orders in the GPWFs. The GPWF for quantum dimer models in three dimensions has already been constructed in Ref. [42]. In three dimensions, the modular group of the 3-torus is $SL(3,\mathbb{Z})$ generated by

$$\hat{S} = \begin{pmatrix} 0 & 1 & 0 \\ 0 & 0 & 1 \\ 1 & 0 & 0 \end{pmatrix}, \quad \hat{T} = \begin{pmatrix} 1 & 0 & 0 \\ 1 & 1 & 0 \\ 0 & 0 & 1 \end{pmatrix}. \quad (18)$$

We can use the UWFO to directly study the topological information in 3+1D [16].

In conclusion, we use the universal wave-function overlap method to exact the modular S and T matrices for the topological order in the Gutzwiller-projected parton wave function for the chiral spin liquid state on the square lattice. The chiral spin liquid is the lattice analogy of the $\nu = \frac{1}{2}$ bosonic Laughlin state, and the analogy is directly confirmed by the modular S and T matrices from the universal wave-function overlap. The exponents in the prefactors of the wave-function overlaps are found to be small, and the variational Monte Carlo calculations are carried out on relatively large systems. The Monte Carlo calculations of the universal wave-function overlap can be easily generalized to other Bravais lattices and 3+1D topological orders.

X-G.W. is supported by NSF Grant No. DMR-1005541 and NSFC 11274192. He is also supported by the BMO Financial Group and the John Templeton Foundation. Research at the Perimeter Institute is supported by the Government of Canada through Industry Canada and by the Province of Ontario through the Ministry of Research.

[1] X. G. Wen, Int. J. Mod. Phys. B **04**, 239 (1990).
[2] X. G. Wen, Phys. Rev. B **40**, 7387 (1989).
[3] X. G. Wen and Q. Niu, Phys. Rev. B **41**, 9377 (1990).
[4] M. Levin and X.-G. Wen, Phys. Rev. Lett. **96**, 110405 (2006).
[5] A. Kitaev and J. Preskill, Phys. Rev. Lett. **96**, 110404 (2006).
[6] X. Chen, Z.-C. Gu, and X.-G. Wen, Phys. Rev. B **82**, 155138 (2010).
[7] X. Wen, *Quantum Field Theory of Many-Body Systems: From the Origin of Sound to an Origin of Light and Electrons*, Oxford Graduate Texts (Oxford University Press, Oxford, 2004).
[8] R. B. Laughlin, Phys. Rev. Lett. **50**, 1395 (1983).
[9] F. Wilczek and A. Zee, Phys. Rev. Lett. **52**, 2111 (1984).
[10] D. Arovas, J. R. Schrieffer, and F. Wilczek, Phys. Rev. Lett. **53**, 722 (1984).
[11] X.-G. Wen, Int. J. Mod. Phys. B **6**, 1711 (1992).
[12] X.-G. Wen, Adv. Phys. **44**, 405 (1995).
[13] E. Keski-Vakkuri and X.-G. Wen, Int. J. Mod. Phys. B **07**, 4227 (1993).
[14] X.-G. Wen, arXiv:1212.5121 [cond-mat.str-el].
[15] F. Liu, Z. Wang, Y.-Z. You, and X.-G. Wen, arXiv:1303.0829 [cond-mat.str-el].
[16] H. Moradi and X.-G. Wen, arXiv:1401.0518 [cond-mat.str-el].
[17] H. He, H. Moradi, and X.-G. Wen, Phys. Rev. B **90**, 205114 (2014).
[18] Z. Wang, *Topological Quantum Computation* (American Mathematical Society, Providence, 2010).
[19] E. Verlinde, Nucl. Phys. B **300**, 360 (1988).
[20] I. Affleck, Phys. Rev. Lett. **56**, 746 (1986).
[21] Y. Zhang, T. Grover, A. Turner, M. Oshikawa, and A. Vishwanath, Phys. Rev. B **85**, 235151 (2012).
[22] L. Cincio and G. Vidal, Phys. Rev. Lett. **110**, 067208 (2013).
[23] H.-H. Tu, Y. Zhang, and X.-L. Qi, Phys. Rev. B **88**, 195412 (2013).
[24] M. P. Zaletel, R. S. K. Mong, and F. Pollmann, Phys. Rev. Lett. **110**, 236801 (2013).
[25] W. Zhu, D. N. Sheng, and F. D. M. Haldane, Phys. Rev. B **88**, 035122 (2013).
[26] Y. Zhang and X.-L. Qi, Phys. Rev. B **89**, 195144 (2014).
[27] Y. Tserkovnyak and S. H. Simon, Phys. Rev. Lett. **90**, 016802 (2003).
[28] E. Kapit, P. Ginsparg, and E. Mueller, Phys. Rev. Lett. **108**, 066802 (2012).
[29] Y.-L. Wu, B. Estienne, N. Regnault, and B. A. Bernevig, Phys. Rev. Lett. **113**, 116801 (2014).

[30] L.-Y. Hung and X.-G. Wen, Phys. Rev. B **89**, 075121 (2014).
[31] X. G. Wen, F. Wilczek, and A. Zee, Phys. Rev. B **39**, 11413 (1989).
[32] V. Kalmeyer and R. B. Laughlin, Phys. Rev. Lett. **59**, 2095 (1987).
[33] X. G. Wen, Phys. Rev. B **44**, 2664 (1991).
[34] X.-G. Wen, Phys. Rev. B **60**, 8827 (1999).
[35] D. F. Schroeter, E. Kapit, R. Thomale, and M. Greiter, Phys. Rev. Lett. **99**, 097202 (2007).
[36] H. Yao and S. A. Kivelson, Phys. Rev. Lett. **99**, 247203 (2007).
[37] F. D. M. Haldane and E. H. Rezayi, Phys. Rev. B **31**, 2529 (1985).
[38] Q. Niu, D. J. Thouless, and Y.-S. Wu, Phys. Rev. B **31**, 3372 (1985).
[39] J.-W. Mei and X.-G. Wen, arXiv:1407.0869 [cond-mat.str-el].
[40] Z.-X. Liu, J.-W. Mei, P. Ye, and X.-G. Wen, Phys. Rev. B **90**, 235146 (2014).
[41] Y. Zhang, T. Grover, and A. Vishwanath, Phys. Rev. B **84**, 075128 (2011).
[42] V. Ivanov, Y. Qi, and L. Fu, Phys. Rev. B **89**, 085128 (2014).